

Supplementary Materials for
**Eliciting the mitochondrial unfolded protein response via NAD⁺
repletion reverses fatty liver disease**

Karim Gariani*, Keir J. Menzies*, Dongryeol Ryu, Casey J. Wegner, Xu Wang, Eduardo R. Ropelle, Norman Moullan, Hongbo Zhang, Alessia Perino, Vera Lemos, Bohkyung Kim, Young-Ki Park, Alessandra Piersigilli, Tho X. Pham, Yue Yang, Chai Siah Ku, Sung I. Koo, Anna Fomitchova, Carlos Cantó, Kristina Schoonjans, Anthony A. Sauve, Ji-Young Lee[#], Johan Auwerx[#].

* These authors contributed equally to this work

To whom correspondence should be addressed: Johan Auwerx (admin.auwerx@epfl.ch) and Ji-Young Lee (ji-young.lee@uconn.edu)

This Doc file includes:

Methods

Figure legends S1 to S5

References

Methods

Animal Experiments.

In vivo phenotyping. Most mouse phenotyping experiments were carried out according to the standard operational procedures (SOPs) guidelines established and validated within the Eumorphia program (1). Body weight and food intake were monitored weekly on the same day. Body composition was determined by Echo-MRI (Echo Medical Systems). Oral glucose tolerance test (OGTT) was performed in mice fasted overnight. Tail vein glucose levels were measured using a Bayer Contourè glucometer immediately before glucose administration and 15, 30, 60, 90 and 120 minutes after glucose administration (1g glucose/kg body weight). Plasma insulin levels from before glucose administration and 15, 30 and 60 min after glucose administration during the OGTT procedure was quantified from heparinized plasma samples using specific ELISA kits (Mercodia). Insulin tolerance test (ITT) was performed on mice fasted for 5 hrs. Tail vein glucose levels were measured using a Bayer Contourè glucometer immediately before Intraperitoneal insulin injection (0.5 units/Kg) and 15, 30, 60, 90 and 120 minutes after insulin injection.

Oxygen consumption (VO_2), carbon dioxide production (VCO_2), feeding activities and activity levels were monitored during the indirect calorimetry tests using the comprehensive laboratory animal monitoring system (CLAMS, Columbus Instruments). The mice were kept in individual cages inside a CLAMS chamber for 2 days; the first day and night was a non-recording adjustment period followed by a 24-h recording at room temperature (+22°C). Measurements were performed for a total of 37 mice (n = 10 on NR, n=10 on HFHS and n= 17 on CD) The results of O_2 consumption and CO_2 production were used to calculate respiratory exchange rate (RER) and analyzed separately from the light (inactive) and dark (active) periods of the day.

Animal sacrifice. After a 4 hours fasting period, mice were anesthetized with sodium pentobarbital (i.p. injection, 50 mg/kg body weight) and euthanized by blood sampling via cardiac puncture. Plasma was collected and frozen at -80°C following centrifugation of heparinized blood samples (2000 rcf for 5 minutes at 4°C). All plasma parameters were measured using a Cobas c111 (Roche Diagnostics). Tissues were snap frozen in liquid nitrogen and together with the plasma stored at -80°C.

NR supplemented food

The NR supplemented pellets were prepared by mixing powdered diet with water only or NR dissolved in water. Pellets were dried under a laminar flow hood at least over night and frozen until needed.

Morphologic analysis

Liver samples, taken from the same lobe of each animal, were fixed in buffered formalin (4%) overnight and embedded in paraffin. 5 μ m thick serial sections were made from paraffin embedded tissue then stained with hematoxylin and eosin (H&E), Picrosirius red and Masson's trichrome to assess fibrosis and collagen, respectively, according to standard protocols. Antigen retrieval was performed on sections before immunohistochemistry. Hydrated sections were boiled in a citric acid solution (10 mmol/L trisodium salt dihydrate pH 6.0, 0.5% Tween-20) for 8 minutes or treated for 25 minutes at 37°C with 0.1% Trypsin in 0.05 M/L Tris, pH 7.8 with 0.1% CaCl. Post-retrieval, slides were stained for CD45 at 1:100 (BD Pharmingen, 30-F11) as a marker of inflammation. Another set of liver samples, taken from the same lobe of each animal, were embedded in Thermo Scientific™ Shandon™ Cryomatrix™ embedding resin and snap-frozen, for 2 minutes in isopentane cooled in liquid nitrogen, before being placed on dry ice. Serial 5 μ m thick cryosections were stained with Oil Red O to assess lipid accumulation, succinate dehydrogenase and cytochrome c oxidase activity as previously described (2).

The histopathological scoring for the severity and extension of hepatocellular steatosis was performed in a blinded fashion by a board certified veterinary pathologist on 5 µm thick sections stained with Hematoxylin and Eosin. A Leica DM500 light microscope (Leica Microsystems, Wetzlar Germany) was used for this purpose. The analysis included the semi-quantitative evaluation of the severity of infiltration according to the parameters reported in Table S2. The overall value of fatty infiltration per animal was the result of the sum or partial scores. Hepatomegaly was also identified, subgrossly, based on sharpness of the natural borders of the organ included in the section.

Respirometry on fresh liver tissue

Mitochondrial function in fresh liver tissue was evaluated using high-resolution respirometry (Oroboros Oxygraph-2k; Oroboros Instruments, Austria), as previously described (3), with minor modifications. Briefly, Complex I driven oxidative phosphorylation was measured by adding malate (1.6 mM), glutamate (20 mM), pyruvate (9.8 mM) and ADP (4.8 mM), followed by the addition of succinate (9.6 mM) to stimulate complex I + complex II driven coupled respiration. Finally, electron transport through complexes I inhibited by sequential addition of rotenone (0.1 mM) (ETS Complex II). O₂ flux obtained in each step of the protocol was normalized by the protein content of the liver sample used for the analysis.

Citrate synthase activity measurement.

Citrate synthase activity was measured following the protocol of Sigma's Citrate Synthase Assay Kit (Sigma-Aldrich, St. Louis, MO, USA).

Western blotting

Protein was extracted using lysis buffer (50 mM Tris, 150 mM KCl, EDTA 1 mM, NP40 1%, nicotinamide 5mM, sodium butyrate 1mM, protease inhibitors pH 7,4). Proteins were separated by SDS-PAGE and transferred onto nitrocellulose membranes. Blocking and antibody incubations were performed in 5% BSA. SIRT1, MTC01, SDHA and HSP10 (CPN10) antibodies were from Abcam; Anti-FOXO1 antibody was from Cell Signaling; anti-acetyl-FRKH (FOXO), TOM20 and HSP90 antibodies were from Santa Cruz Inc.; HSP60 antibody was from Enzo Life Science; Antibody cocktail (the Mitoprofile Total OXPHOS Rodent WB Antibody Cocktail) for mitochondrial subunits was purchased from Mitosciences; CLPP antibody was from Sigma. Antibody detection reactions were developed by enhanced chemiluminescence (Advansta, CA, USA) using x-ray films or imaged using the c300 imaging system (Azure Biosystems).

Blue-Native Page

Blue-Native Page was performed using the Native-PAGE™ Novex® Bis-Tris Gel system (Invitrogen). Briefly, 50µg of mitochondria was isolated, as previously described (4), then solubilized using Native-PAGE sample buffer with 0.5% n-dodecyl-β-D-maltoside (Invitrogen). Mitochondrial complexes were separated using a Native-PAGE Novex 3–12% Bis- Tris gel (Invitrogen) and transferred to a PVDF membrane using the iBlot™ Gel Transfer System (Invitrogen). The membrane was then fixed with 8% acetic acid, dried overnight, and destained with methanol. To detect OXPHOS complexes, the membrane was stained with the Mitoprofile Total OXPHOS Rodent WB Antibody Cocktail (Mitosciences). The membrane was then washed and the signal was detected using the Western Breeze® Chromogenic Western Blot Immunodetection Kit (Invitrogen).

Quantitative real-time qPCR for mRNA and DNA quantification

Total RNA was prepared using TRIzol (Invitrogen) according to the manufacturer's instructions. RNA was treated with DNase, and 2 µg of RNA was used for reverse transcription (RT). 10X diluted cDNA was used for RT-quantitative PCR (RT-qPCR) reactions. The RT-qPCR reactions were performed using the Light-Cycler system (Roche Applied Science) and a qPCR Supermix (Qiagen) with the indicated primers. Data was normalized using 36B4. The average of at least three technical repeats was used for each biological data point. Primer sequences are shown in Table S3.

To measure mtDNA content (marker of mitochondrial number), liver tissue was homogenized using 1x PBS and digested in a lysis buffer containing Proteinase K overnight. Genomic and mitochondrial DNA were extracted by conventional phenol-chloroform method. Then quantitative PCR was performed using mitochondrial DNA (*Cox2*) and genomic DNA (*Hk2*) specific primers Table S3 as previously described (5).

Supplementary Figures

Fig. S1

(A) Transcripts from NAD⁺-synthesis genes (shown in blue font), in contrast to NAD⁺-consuming genes (shown in red font), were positively correlated with regulators of β -oxidation using a matching custom designed data-sets derived from two human data sets, including 427 (6) and 220 (7) human liver samples or two mouse data sets, including 42 BXD strains fed either chow or high-fat diets (8, 9). These matching data-sets further complement data from figures 1A and 1B and emphasize the conservation of these correlations. As seen on a correlogram, blue correlations are positive and red correlations are negative (intensity reflects significance).

Fig. S2

(A) Schematic illustrating the experimental design for indirect calorimetry tests (CLAMS) that were performed on CD, HFHS and NR-Prev cohorts, following 5 weeks of treatment (NR dose: 400 mg/kg/day). The NR-Ther cohort is not included in this measurement since these animals did not yet start their NR treatment. Compared to the HFHS cohort, the respiratory exchange ratio (RER), total VO₂ and total VCO₂ demonstrated an increased use of lipids during the (B) dark and (C) light cycles upon NR treatment. Animals fed HFHS or NR/HFHS showed similar levels of activity throughout the measurements (n=8-10). * $P < 0.05$, ** $P < 0.001$, *** $P < 0.0001$ compared to the HFHS cohort. Data are expressed as mean \pm s.e.m. One-way ANOVA with a *post-hoc* Bonferroni test was used for all statistical analyses. Male mice were used for these experiments.

Fig. S3

CD, HFHS, NR-Prev and NR-Ther cohorts following 5-17-weeks of treatment (NR dose: 400 mg/kg/day). (A) Images of liver sections were stained with Masson's Trichrome (collagen appears blue) or CD45 antibody to highlight leukocytes from non-hematopoietic cells (CD45 positive appears brown) (n=3). Male mice were used for these experiments.

Fig. S4

(A) SiRNA knockdown of *Ppar δ / β* in vehicle (ddH₂O) or NR (1mM) treated AML12 cells altered mRNA transcript levels of *Sirt1*, β -oxidation genes (*Mcad*, *Cpt1* and *Acox1*) and mitochondrial biogenesis genes (*Pgc1 α* , *Tfam*, *Nrf1*, *Cox2* and *Tomm40*). * $P < 0.05$ compared to the indicated group and ϵ , $P < 0.05$, overall effect of treatment versus control mice, \ddagger , $P < 0.05$, interaction of each treatment versus control mice. Two-way ANOVA with a *post-hoc* Holm-Sidak test was used for statistical analyses. Data are expressed as mean \pm s.e.m.

Fig. S5

(A) SIRT1 inhibition with the SIRT1 inhibitor EX527 (10 μ M) in AML12 hepatoma cells attenuated increases in mitochondrial proteins and reductions in FOXO1 acetylation levels following NR treatment. (B) Combining NR treatment of *Sirt3*^{L2/L2} hepatocytes with infection with an adenovirus expressing either *Gfp* or *Cre* attenuated mitochondrial protein expression upon *Sirt3* loss-of-function. The presence of the mitonuclear imbalance and the activation of the UPR^{mt} is demonstrated by the unequal changes in SDHB and MTCO1 expression and by the increase in HSP10, respectively. These effects are also shown to be dependent on SIRT1. Male mice were used for these experiments.

References

1. Champy MF, Selloum M, Zeitler V, Caradec C, Jung B, Rousseau S, Pouilly L, et al. Genetic background determines metabolic phenotypes in the mouse. *Mamm Genome* 2008;19:318-331.
2. Yamamoto H, Williams EG, Mouchiroud L, Cantó C, Fan W, Downes M, Héligon C, et al. NCoR1 Is a Conserved Physiological Modulator of Muscle Mass and Oxidative Function. *Cell* 2011;147:827-839.
3. Boushel R, Gnaiger E, Schjerling P, Skovbro M, Kraunsøe R, Dela F. Patients with type 2 diabetes have normal mitochondrial function in skeletal muscle. *Diabetologia* 2007;50:790-796.
4. Frezza C, Cipolat S, Scorrano L. Organelle isolation: functional mitochondria from mouse liver, muscle and cultured fibroblasts. *Nat Protoc* 2007;2:287-295.
5. Lagouge M, Argmann C, Gerhart-Hines Z, Meziane H, Lerin C, Daussin F, Messadeq N, et al. Resveratrol improves mitochondrial function and protects against metabolic disease by activating SIRT1 and PGC-1alpha. *Cell* 2006;127:1109-1122.
6. Schadt EE, Molony C, Chudin E, Hao K, Yang X, Lum PY, Kasarskis A, et al. Mapping the genetic architecture of gene expression in human liver. *PLoS biology* 2008;6:e107.
7. Tummala KS, Gomes AL, Yilmaz M, Graña O, Bakiri L, Ruppen I, Ximénez-Embún P, et al. Inhibition of De Novo NAD(+) Synthesis by Oncogenic URI Causes Liver Tumorigenesis through DNA Damage. *Cancer cell* 2014;26:826-839.
8. Pirinen E, Canto C, Jo YS, Morato L, Zhang H, Menzies KJ, Williams EG, et al. Pharmacological Inhibition of poly(ADP-ribose) polymerases improves fitness and mitochondrial function in skeletal muscle. *Cell Metab* 2014;19:1034-1041.
9. Williams EG, Mouchiroud L, Frochoux M, Pandey A, Andreux PA, Deplancke B, Auwerx J. An evolutionarily conserved role for the aryl hydrocarbon receptor in the regulation of movement. *PLoS Genetics* 2014;10:e1004673.

Table S1. Modified AIN-93M diet

Ingredient	LF	HFC	NR-Ther
		<i>g/Kg diet</i>	
Cornstarch	620.70	168.70	168.70
Sucrose	100.00	340.00	340.00
Casein	140.00	170.00	170.00
Lard	0.00	190.00	190.00
Soybean oil	40.00	30.00	30.00
Cholesterol	0.00	1.85	1.85
Fiber ¹	40.00	40.00	40.00
Guar gum	10.00	10.00	10.00
Mineral mix ²	35.00	35.00	35.00
Vitamin mix ³	10.00	10.00	10.00
L-Cystine	1.80	1.80	1.80
t-Butylhydroquinone	0.01	0.01	0.01
Choline bitartrate	2.50	2.50	2.50
Nicotinamide riboside	0.00	0.00	500 mpk

¹Solka-Floc cellulose; ²AIN-93 mineral mix; ³AIN-93 vitamin mix.

Table S2. Parameters for evaluation of steatosis in liver histological sections.

Severity	0 = absent; 1 = 2-3 vacuoles per hepatic cord per lobule; 2 = less than half of the lobule has fatty vacuolation 3 = more than half of the lobule has fatty vacuolation 4 = almost the entire lobule has fatty infiltration
Extension	Focal = 1 Multifocal = 2 Diffuse = 3

Table S3. Primer list for RT-qPCR

Gene	Forward primer	Reverse primer
<i>36b4</i>	AGATTCGGGATATGCTGTTGG	AAAGCCTGGAAGAAGGAGGTC
<i>Sirt1</i>	GTCTCCTGTGGGATTCCTGA	ACACAGAGACGGCTGGAAC
<i>Tfam</i>	AAGTGTTCCTCCAGCATGGG	GGCTGCAATTTTCCTAACCA
<i>Erra</i>	ACTGCCACTGCAGGATGAG	CACAGCCTCAGCATCTTCAA
<i>Mcad</i>	GATCGCAATGGGTGCTTTTGATAGAA	AGCTGATTGGCAATGTCTCCAGCAAA
<i>Pgc1α</i>	AAGTGTGGAACCTCTCTGGAAC	GGGTTATCTTGGTTGGCTTTATG
<i>Cpt1b</i>	CCCATGTGCTCCTACCAGAT	CCTTGAAGAAGCGACCTTTG
<i>Scd1</i>	GAGGCCTGTACGGGATCATA	CCGAAGAGGCAGGTGTAGAG
<i>Acox1</i>	GCCCAACTGTGACTTCCATT	GGCATGTAACCCGTAGCACT
<i>Cox5a</i>	GAGCCCAAATCATTGATGC	TGAGGTCCTGCTTTGTCCTT
<i>Timm17a</i>	GCGGCATTCTCCTAGCTTTA	CTGTGCGTAGTCTCCAAACG
<i>Nrf1</i>	CGGAGTGACCCAACTGAAC	GATGACCACCTCGACCGTTT
<i>Tomm40</i>	CCAGAGCATCACACCGTGTC	CCAGCGTTACTGTAGCCAACC
<i>Tomm20</i>	GCCCTCTTCATCGGGTACTG	ACCAAGCTGTATCTCTTCAAGGA
<i>Acc1</i>	GACAGACTGATCGCAGAGAAAG	TGGAGAGCCCCACACACA
<i>Fasn</i>	AGCTTCGGCTGCTGTTGGAAGT	TCGGATGCCTCTGAACCACTCACA
<i>Srebf1</i>	GGCACTAAGTGCCCTCAACCT	GCCACATAGATCTCTGCCAGTGT
<i>Mcp1</i>	AGGTCCCTGTATGCTTCTG	GCTGCTGGTGATCCTCTTGT
<i>Vcam</i>	GACTCTGGAGTCTATGTGTGTGAAGG	TCAGAACAACCGAATCCCCA
<i>Tnfa</i>	GGGACAGTGACCTGGACTGT	AGGCTGTGCATTGCACCTCA
<i>Ndufs1</i>	AGGATATGTTGCGACAACCTGG	TCATGGTAACAGAATCGAGGGA
<i>Nampt</i>	CCGCCACAGTATCTGTTCCCTT	AGTGGCCACAAATTCCAGAGA
<i>Cox2</i>	TTCCAATCCATGTCAAACCGT	CTGGTCAAATCCTGTGCTCAT
<i>Ppara</i>	AGGAAGCCGTTCTGTGACAT	TTGAAGGAGCTTTGGGAAGA
<i>Pparδ/β</i>	AATGCGCTGGAGCTCGATGAC	ACTGGCTGTCAGGGTGGTTG
<i>Pparγ</i>	CCACCAACTTCGGAATCAGCT	TTTGTGGATCCGGCAGTTAAGA
<i>Dgat1</i>	GTGGCTGCATTTAGATTGAG	CACAGCTATCAGCCAGCAGTC
<i>Apob</i>	GCCCATTGTGGACAAGTTGATC	CCAGGACTTGGAGGTCTTGA
<i>Clpp</i>	TGTTGCGGGAACGCATCGTGT	AGATGGCCAGGCCCGCAGTT
<i>Hspe1</i>	CTGACAGGTTCAATCTCTCCAC	AGGTGGCATTATGCTTCCAG
<i>Hspd1</i>	GCTGTAGCTGTTACAATGGGG	TGACTTTGCAACAGTGACCC
<i>Cox2</i>	GTTGATAACCGAGTCGTTCTGC	CCTGGGATGGCATCAGTTTT
<i>Hk2</i>	GCCAGCCTCTCCTGATTTTAGTGT	GGGAACACAAAAGACCTCTTCTGG
<i>Atf4</i>	TGAAGGAGTTCGACTTGGATGCC	CAGAAGGTCATCTGGCATGGTTTC
<i>Chop</i>	GTCCCTAGCTTGGCTGACAGA	TGGAGAGCGAGGGCTTTG
<i>Grp78</i>	ACTTGGGGACCACCTATTCCT	ATCGCCAATCAGACGCTCC
<i>Xbp1s</i>	AAGAACACGCTTGGGAATGG	CTGCACCTGCTGCGGAC
<i>Xbp1m</i>	AGCAGCAAGTGGTGGATTTG	GAGTTTCTCCCATAAAAGCTGA
<i>Cd36</i>	GATGTGGAACCCATAACTGGATTCAC	GGTCCCAGTCTCATTTAGCCACAGTA
<i>Cideb</i>	GACGACACGTGCTTGTGATGGT	GTCTCGGGGATTTTGCTTGTGA
<i>Il-1b</i>	CAACCAACAAGTGATATTCTCCATG	GATCCACACTCTCCAGCTGCA
<i>Il-6</i>	GCTACCAAACCTGGATATAATCAGGAAA	CTTGTTATCTTTAAGTTGTTCTTCATGTA
<i>Col</i>	TAGGCCATTGTGTATGCAGC	ACATGTTGAGCTTTGTGGACC
<i>Fn1</i>	ACTGGATGGGGTGGGAAT	GGAGTGGCACTGTCAACCTC
<i>Acta2</i>	CCCAGACATCAGGGAGTAATGG	TCTATCGGATACTTCAGCGTCA

FIGURE S1

A

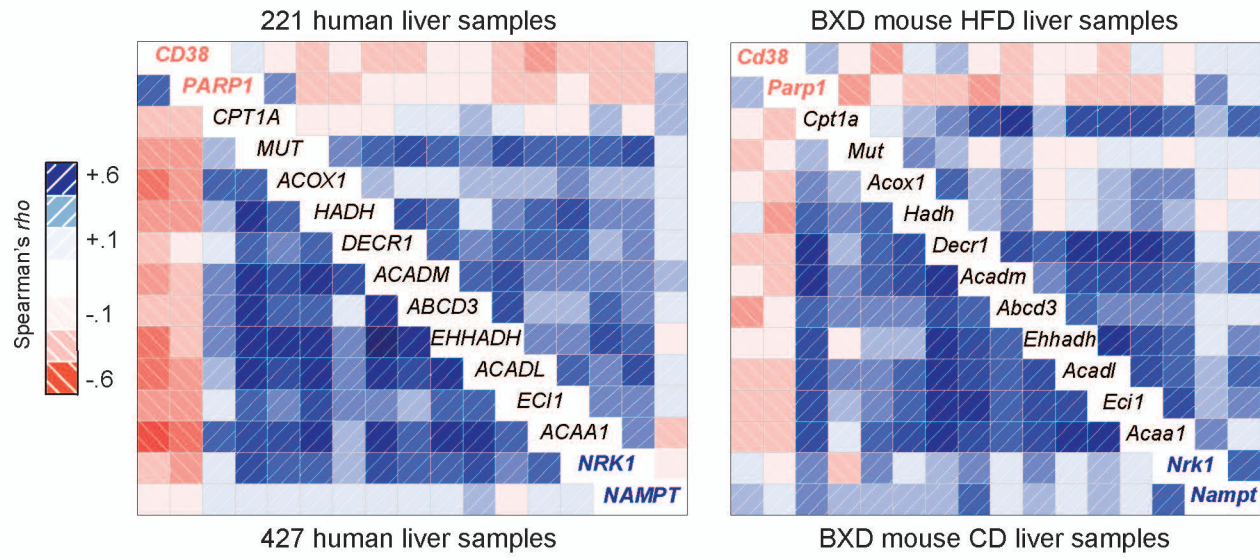


FIGURE S2

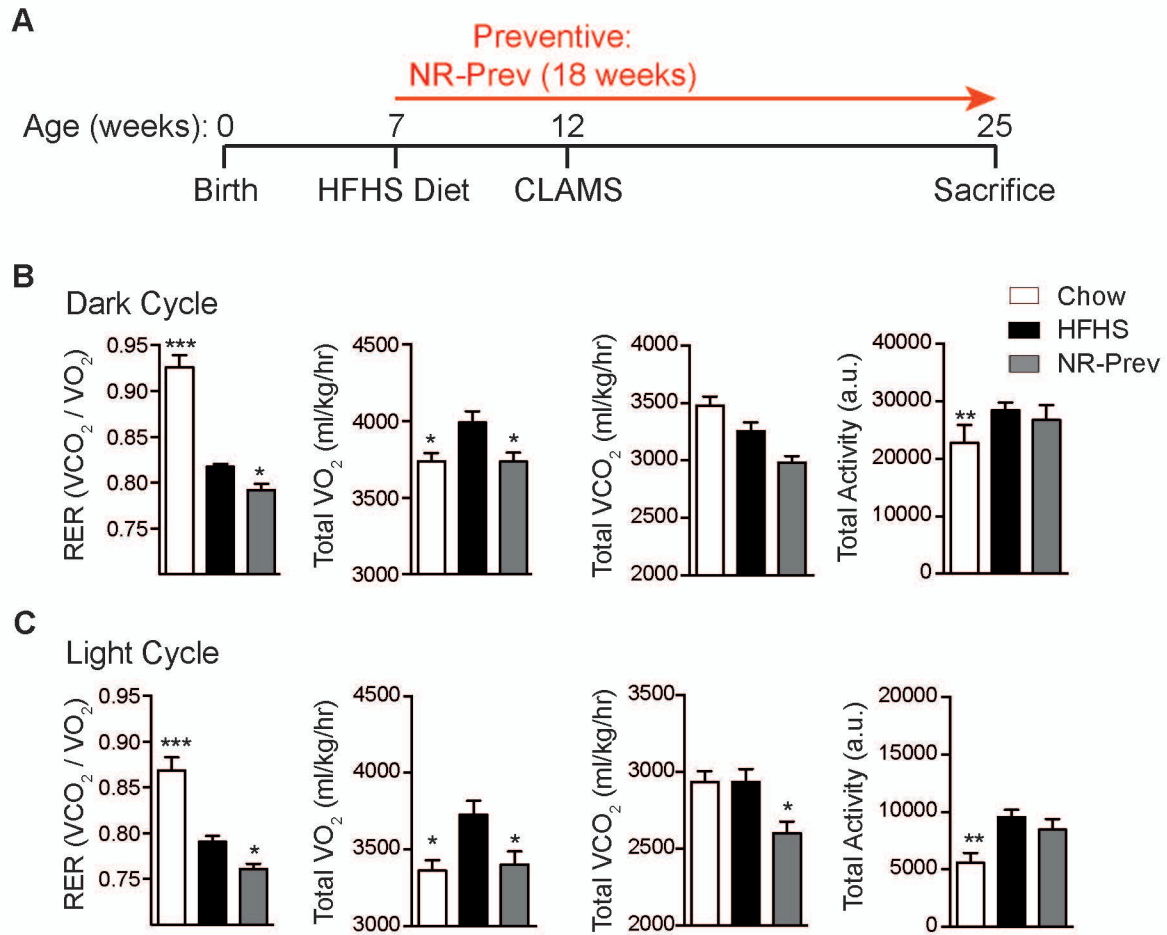


FIGURE S3

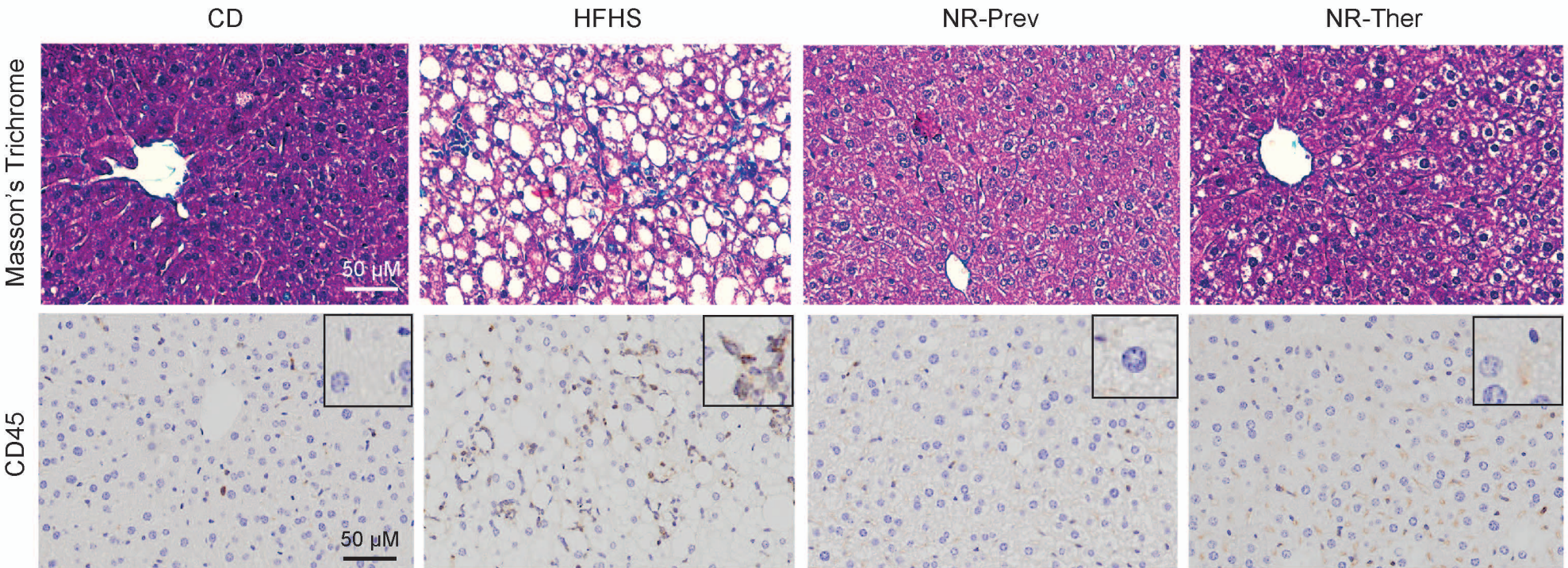


FIGURE S4

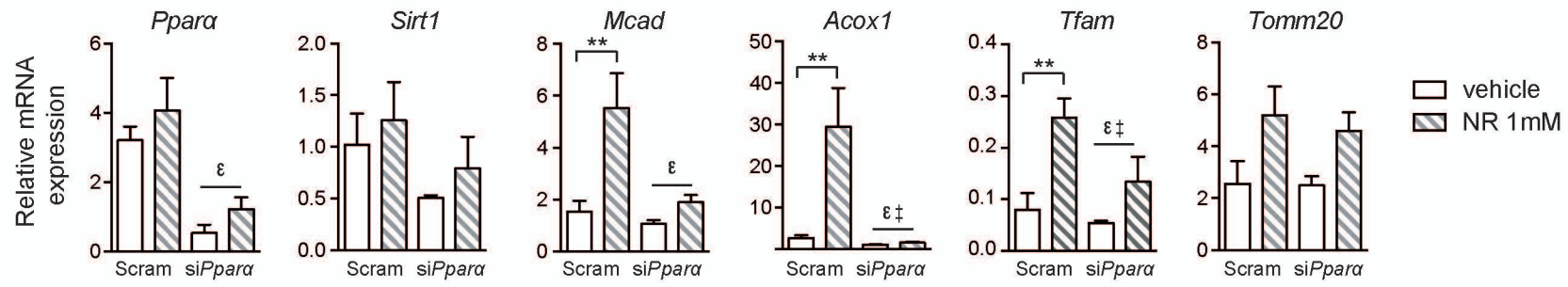


FIGURE S5

